Nonlinear Dyn (2010) 59: 161–172
DOI 10.1007/s11071-009-9529-5

ORIGINAL PAPER

Rich dynamics in a non-local population model over three patches

Peixuan Weng · Cuntao Xiao · Xingfu Zou

Received: 6 December 2007 / Accepted: 6 May 2009 / Published online: 22 May 2009

Abstract We consider a system of nonlinear delay differential equations that describes the growth of the mature population of a species with age-structure living over three patches. We analyze existence of non-negative homogeneous equilibria and their stability and discuss possible Hopf bifurcation from these equilibria. More precisely, by employing both the standard Hopf bifurcation theory and the symmetric bifurcation theory for functional differential equations, we obtain very rich dynamics for the system, including bistable equilibria, transient oscillations, synchronous periodic solutions, phase-locked periodic solutions, mirror-reflecting waves and standing waves.

Keywords Non-local model · Delay · Symmetric functional differential equation · Homogeneous equilibria · Hopf bifurcation · Periodic solutions · Stability

Research of P. Weng was supported by Natural Science Foundation of China (10571064), Guangdong Natural Science Foundation (04010364), and China Scholarship Council. Research of X. Zou was supported by NSERC of Canada, by MITACS-NCE and by a Premier's Research Excellence Award of Ontario.

P. Weng
Department of Mathematics, South China Normal University, Guangzhou 510631, People's Republic of China
e-mail: wengpx@scnu.edu.cn

C. Xiao
Department of Mathematics, Guangdong University of Technology, Guangzhou 510090, People's Republic of China
e-mail: xiaocuntao@sohu.com

X. Zou (✉)
Department of Applied Mathematics, University of Western Ontario, London, Ontario N6A 5B7, Canada
e-mail: xzou@uwo.ca

1 Introduction

Recently, So et al. [10] derived a model for a single species living in two patches with age-structure, and investigated existence and stability of non-negative homogeneous equilibria, and the Hopf bifurcation from them. Under some suitable conditions on the maturation age r, the mature and immature dispersal rates D_m and D_I, the mature and immature death rates d_m and d_I, they observed that the transient oscillations may occur near the intermediate equilibrium. Near the largest positive equilibrium, synchronized periodic oscillations and unstable phase-locked oscillations may occur simultaneously. Stability and the bifurcation direction of the periodic waves from Hopf bifurcation were not discussed in, and as was pointed out in, the global dynamics of the model is far from being completely understood at this moment.

The system in [10] consists of only two equations, and the characteristic equation at an equilibrium has the form

$$\left(\lambda + k_1 + l_1 e^{-\lambda r}\right)\left(\lambda + k_2 + l_2 e^{-\lambda r}\right) = 0,$$

where $k_i, l_i, i = 1, 2,$ and r are known constants. Therefore, every possible pair of purely imaginary roots of the characteristic equation is simple, and hence, the standard Hopf bifurcation theorem for functional differential equations (cf. Hale and Verduyn Lunel [5], Hassard et al. [6]) can be applied.

However, if the number of the patches $n \geq 3$, things would be different. Taking $n = 3$ as an example, we encounter a system of three equations. In this situation, the characteristic equation at an equilibrium will be of the form

$$\left(\lambda + k_1 + l_1 e^{-\lambda r}\right)\left(\lambda + k_2 + l_2 e^{-\lambda r}\right)^2 = 0,$$

which may have purely imaginary roots that are not simple, and thus, the standard Hopf bifurcation theorem of functional differential equations does not apply. In this paper, we shall generalize the work of [10] to the situation with three patches. Although the derivation of the model equations is similar to that in [10], for readers' convenience, we give it in Sect. 2. In Sect. 3, we analyze existence of possible homogeneous equilibria and their stability, as well as Hopf bifurcations from these equilibria. Depending on whether the purely imaginary roots are simple or multiple, we apply, respectively, the standard Hopf bifurcation theory or the symmetric Hopf bifurcation theory for functional differential equations. Interestingly, by applying a theorem from [12], we obtain coexistence of phase-locked oscillations, mirror-reflecting waves and standing waves. The results in this paper, compared with those in [10], clearly show how the number of patches would enrich the dynamics of the model systems.

We point out that the model in this paper and the one in [10] are both spatially non-local. Such non-locality is a result of the maturation delay and the mobility of the immature population, and thus, reflects the duality of the time and space in nature. We would also like to mention that the symmetric bifurcation theory for functional differential equations has been recently applied to a variety of model equations from population biology and neural networks to obtain existence of various periodic solutions with certain symmetries, including phase-locked oscillations, mirror-reflecting waves and standing waves (see, e.g., [1–4, 7, 8, 11–15] and the references therein).

2 Model derivation

Consider the population of a single species distributed over three patches. Let $u_i(t, a)$ be the population density of the species of age a $(0 < a < \infty)$ in patch i $(i = 1, 2, 3)$ at time t $(t \geq 0)$. In view of [9], we have

$$\begin{cases} \frac{\partial u_1(t,a)}{\partial t} + \frac{\partial u_1(t,a)}{\partial a} \\ \quad = -d_1(a)u_1(t,a) + D_{21}(a)u_2(t,a) \\ \qquad + D_{31}(a)u_3(t,a) - D_{12}(a)u_1(t,a) \\ \qquad - D_{13}(a)u_1(t,a), \\ \frac{\partial u_2(t,a)}{\partial t} + \frac{\partial u_2(t,a)}{\partial a} \\ \quad = -d_2(a)u_2(t,a) + D_{12}(a)u_1(t,a) \\ \qquad + D_{32}(a)u_3(t,a) - D_{21}(a)u_2(t,a) \\ \qquad - D_{23}(a)u_2(t,a), \\ \frac{\partial u_3(t,a)}{\partial t} + \frac{\partial u_3(t,a)}{\partial a} \\ \quad = -d_3(a)u_3(t,a) + D_{13}(a)u_1(t,a) \\ \qquad + D_{23}(a)u_2(t,a) - D_{31}(a)u_3(t,a) \\ \qquad - D_{32}(a)u_3(t,a), \end{cases} \tag{2.1}$$

where the non-negative functions $d_i(a)$ $(i = 1, 2, 3)$ are the death rates of the individuals of age a in patch i respectively, and the non-negative functions $D_{ij}(a)u_i(t, a)$ with $j \neq i$ correspond to the dispersal of the species at age a from patch i to patch j, $1 \leq i \neq j \leq 3, i = 1, 2, 3$. We also assume that there is no loss during migration from patch i to patch j.

Suppose that the population consists of two age-structure groups: immature and mature, and denote the maturation age by $r > 0$. For simplicity, we assume that, for $i, j = 1, 2, 3$,

$$d_i(a) = \begin{cases} d_{i,I}(a) = d_I(a), & 0 \leq a \leq r, \\ d_{i,m}(a) \equiv d_m, & a > r; \end{cases} \tag{2.2}$$

and

$$D_{ij}(a) = \begin{cases} D_{ij,I}(a) = D_I(a), & 0 \leq a \leq r, \\ D_{ij,m}(a) \equiv D_m, & a > r. \end{cases} \tag{2.3}$$

Here d_m and D_m are constants, I and m stand for immature and mature respectively. Then, the adult (mature) population in the ith patch is given by

$$w_i(t) = \int_r^\infty u_i(t,a)\,da. \tag{2.4}$$

Since only adults can give birth, we have

$$u_i(t,0) = b_i\big(w_i(t)\big). \tag{2.5}$$

Here $b_i(w_i(t))$ is the birth function of the species in the ith patch. It is biologically reasonable to assume that $u_i(t,\infty)=0$. By integrating (2.1) with (2.2) and (2.3), from r to ∞, we obtain

$$\begin{aligned}
\frac{d}{dt}w_i(t) &= -\int_r^\infty \frac{\partial u_i}{\partial a}(t,a)\,da - \int_r^\infty d_i(a)u_i(t,a)\,da\\
&\quad + \sum_{j\neq i}\int_r^\infty D_{ji}(a)u_j(t,a)\,da\\
&\quad - \sum_{j\neq i}\int_r^\infty D_{ij}(a)u_i(t,a)\,da\\
&= u_i(t,r) - d_m w_i(t)\\
&\quad + \sum_{j\neq i} D_m w_j(t) - \sum_{j\neq i} D_m w_i(t)\\
&= -d_m w_i(t) + D_m \sum_{j\neq i} w_j(t)\\
&\quad - 2D_m w_i(t) + u_i(t,r),
\end{aligned} \tag{2.6}$$

which leads to

$$\begin{cases}
\frac{d}{dt}w_1(t) = -d_m w_1(t) + D_m(w_2(t)+w_3(t))\\
\qquad\qquad - 2D_m w_1(t) + u_1(t,r),\\
\frac{d}{dt}w_2(t) = -d_m w_2(t) + D_m(w_1(t)+w_3(t))\\
\qquad\qquad - 2D_m w_2(t) + u_2(t,r),\\
\frac{d}{dt}w_3(t) = -d_m w_3(t) + D_m(w_1(t)+w_2(t))\\
\qquad\qquad - 2D_m w_3(t) + u_3(t,r).
\end{cases} \tag{2.7}$$

In the above, $u_i(t,r)$ accounts for the maturation force from all patches into patch i. We need to express each of $u_i(t,r)$ $(i=1,2,3)$ in terms of w_i, $i=1,2,3$. This can be achieved by the same way as in [10], and we give the details below.

Fix $s\geq -r$, and let

$$V_i^s(t) = u_i(t,t-s), \quad s\leq t\leq s+r \ (i=1,2,3). \tag{2.8}$$

From (2.1) it follows that

$$\begin{aligned}
\frac{d}{dt}V_i^s(t) &= \left[\frac{\partial u_i(t,a)}{\partial t} + \frac{\partial u_i(t,a)}{\partial a}\frac{\partial a}{\partial t}\right]_{a=t-s}\\
&= \left[\frac{\partial u_i(t,a)}{\partial t} + \frac{\partial u_i(t,a)}{\partial a}\right]_{a=t-s}\\
&= -d_i(t-s)V_i^s(t) + \sum_{j\neq i} D_{ji}(t-s)V_j^s(t)\\
&\quad - \sum_{j\neq i} D_{ij}(t-s)V_i^s(t)\\
&= -d_I(t-s)V_i^s(t) + \sum_{j\neq i} D_I(t-s)V_j^s(t)\\
&\quad - 2D_I(t-s)V_i^s(t),
\end{aligned} \tag{2.9}$$

for $t\in[s,s+r]$ and $1\leq i\neq j\leq 3$. Summing up for $i=1,2,3$, we obtain

$$\begin{aligned}
&\frac{d}{dt}\big[V_1^s(t)+V_2^s(t)+V_3^s(t)\big]\\
&\quad = -d_I(t-s)\big[V_1^s(t)+V_2^s(t)+V_3^s(t)\big].
\end{aligned} \tag{2.10}$$

Solving this ODE for $[V_1^s(t)+V_2^s(t)+V_3^s(t)]$ and using (2.5), we have

$$\begin{aligned}
&V_1^s(t)+V_2^s(t)+V_3^s(t)\\
&\quad = e^{\int_s^t -d_I(\theta-s)d\theta}\big[V_1^s(s)+V_2^s(s)+V_3^s(s)\big]\\
&\quad = e^{\int_s^t -d_I(\theta-s)d\theta}\big[u_1(s,0)+u_2(s,0)+u_3(s,0)\big]\\
&\quad \overset{a=\theta-s}{=} e^{-\int_0^{t-s} d_I(a)da}\sum_{i=1}^3 b_i\big(w_i(s)\big).
\end{aligned} \tag{2.11}$$

It follows from (2.8) and (2.9) that

$$\begin{aligned}
&\frac{d}{dt}V_1^s(t)\\
&\quad = -d_I(t-s)V_1^s(t) + D_I(t-s)\big(V_2^s(t)+V_3^s(t)\big)\\
&\qquad - 2D_I(t-s)V_1^s(t)\\
&\quad = -\big[d_I(t-s)+3D_I(t-s)\big]V_1^s(t)\\
&\qquad + D_I(t-s)\big[V_1^s(t)+V_2^s(t)+V_3^s(t)\big]\\
&\quad = -\big[d_I(t-s)+3D_I(t-s)\big]V_1^s(t)\\
&\qquad + D_I(t-s)e^{-\int_0^{t-s} d_I(a)da}\sum_{i=1}^3 b_i\big(w_i(s)\big)\\
&\quad = -D^*(t-s)V_1^s(t)\\
&\qquad + D_I(t-s)e^{-\int_0^{t-s} d_I(a)da}\sum_{i=1}^3 b_i\big(w_i(s)\big),
\end{aligned} \tag{2.12}$$

where $D^*(a)=d_I(a)+3D_I(a)$. Solving this equation gives

$$\begin{aligned}V_1^s(t)&=e^{-\int_0^{t-s}D^*(a)da}b_1\big(w_1(s)\big)\\&\quad+\bigg[\int_s^t e^{-\int_{\xi-s}^{t-s}D^*(a)da}D_I(\xi-s)\\&\quad\times e^{-\int_0^{\xi-s}d_I(a)da}\,d\xi\bigg]\sum_{i=1}^3 b_i\big(w_i(s)\big)\\&=e^{-\int_0^{t-s}D^*(a)da}b_1\big(w_1(s)\big)\\&\quad+e^{-\int_0^{t-s}d_I(a)da}\bigg[\int_s^t e^{-3\int_{\xi-s}^{t-s}D_I(a)da}\\&\quad\times D_I(\xi-s)\,d\xi\bigg]\sum_{i=1}^3 b_i\big(w_i(s)\big),\end{aligned}\tag{2.13}$$

which, together with (2.8), leads to

$$\begin{aligned}u_1(t,r)&=V_1^{t-r}(t)=e^{-\int_0^r D^*(a)da}b_1\big(w_1(t-r)\big)\\&\quad+e^{-\int_0^r d_I(a)da}\bigg[\int_{t-r}^t e^{-3\int_{\xi-t+r}^r D_I(a)da}\\&\quad\times D_I(\xi-t+r)\,d\xi\bigg]\sum_{i=1}^3 b_i\big(w_i(t-r)\big)\\&=e^{-\int_0^r D^*(a)da}b_1\big(w_1(t-r)\big)\\&\quad+e^{-\int_0^r d_I(a)da}\int_0^r e^{-3\int_\theta^r D_I(a)da}D_I(\theta)\,d\theta\\&\quad\times\sum_{i=1}^3 b_i\big(w_i(t-r)\big).\end{aligned}\tag{2.14}$$

Since

$$\begin{aligned}&\int_0^r e^{-3\int_\theta^r D_I(a)da}D_I(\theta)\,d\theta\\&\quad=\frac{1}{3}\int_0^r e^{-3\int_\theta^r D_I(a)da}d\bigg(-3\int_\theta^r D_I(a)\,da\bigg)\\&\quad=\bigg[\frac{1}{3}e^{-3\int_\theta^r D_I(a)da}\bigg]_0^r=\frac{1}{3}\big(1-e^{-3\int_0^r D_I(a)da}\big),\end{aligned}$$

we can further express $u_1(t,r)$ as

$$\begin{aligned}u_1(t,r)&=e^{-\int_0^r D^*(a)da}b_1\big(w_1(t-r)\big)\\&\quad+\frac{1}{3}\big(1-e^{-3\int_0^r D_I(a)da}\big)\\&\quad\times e^{-\int_0^r d_I(a)da}\sum_{i=1}^3 b_i\big(w_i(t-r)\big)\\&=\frac{1}{3}e^{-\int_0^r d_I(a)da}\big(1+2e^{-3\int_0^r D_I(a)da}\big)\\&\quad\times b_1\big(w_1(t-r)\big)\\&\quad+\frac{1}{3}e^{-\int_0^r d_I(a)da}\big(1-e^{-3\int_0^r D_I(a)da}\big)\\&\quad\times\big(b_2\big(w_2(t-r)\big)+b_3\big(w_3(t-r)\big)\big)\\&=\frac{1}{3}\rho(1+2r^*)b_1\big(w_1(t-r)\big)\\&\quad+\frac{1}{3}\rho(1-r^*)\big(b_2\big(w_2(t-r)\big)\\&\quad+b_3\big(w_3(t-r)\big)\big),\end{aligned}\tag{2.15}$$

where

$$\rho=e^{-\int_0^r d_I(a)da},\qquad r^*=e^{-3\int_0^r D_I(a)da}.$$

In a similar way, we can obtain

$$\begin{aligned}u_2(t,r)&=\frac{1}{3}\rho(1+2r^*)b_2\big(w_2(t-r)\big)+\frac{1}{3}\rho(1-r^*)\\&\quad\times\big(b_1\big(w_1(t-r)\big)+b_3\big(w_3(t-r)\big)\big),\end{aligned}\tag{2.16}$$

$$\begin{aligned}u_3(t,r)&=\frac{1}{3}\rho(1+2r^*)b_3\big(w_3(t-r)\big)+\frac{1}{3}\rho(1-r^*)\\&\quad\times\big(b_1\big(w_1(t-r)\big)+b_2\big(w_2(t-r)\big)\big).\end{aligned}\tag{2.17}$$

Finally, substituting (2.15)–(2.17) into (2.7), we arrive at the following model system for the adult population growth in three patches:

$$\begin{cases}\frac{d}{dt}w_1(t)\\\quad=-(d_m+2D_m)w_1(t)+D_m(w_2(t)+w_3(t))\\\qquad+\frac{1}{3}\rho(1+2r^*)b_1(w_1(t-r))\\\qquad+\frac{1}{3}\rho(1-r^*)(b_2(w_2(t-r))+b_3(w_3(t-r))),\\\frac{d}{dt}w_2(t)\\\quad=-(d_m+2D_m)w_2(t)+D_m(w_1(t)+w_3(t))\\\qquad+\frac{1}{3}\rho(1+2r^*)b_2(w_2(t-r))\\\qquad+\frac{1}{3}\rho(1-r^*)(b_1(w_1(t-r))+b_3(w_3(t-r))),\\\frac{d}{dt}w_3(t)\\\quad=-(d_m+2D_m)w_3(t)+D_m(w_1(t)+w_2(t))\\\qquad+\frac{1}{3}\rho(1+2r^*)b_3(w_3(t-r))+\frac{1}{3}\\\qquad\times\rho(1-r^*)(b_1(w_1(t-r))+b_2(w_2(t-r))),\end{cases}\tag{2.18}$$

where $d_m, D_m, b(w), \rho, r^*$ are defined as above. One important feature of this model (as well as the model in [10]) is that the growth rate of the mature population at time t in each patch depends on the births in all patches at a previous time $t-r$, and such a *delayed non-locality* is caused by the dispersion of the immature populations between the three patches.

3 Equilibria, stability and Hopf bifurcation

In general, the analysis of equilibria of (2.18) is difficult. In this section, we assume that the birth functions for the three patches are identical, that is, $b_i(w) = b(w), i = 1, 2, 3$. Then (2.18) becomes

$$\begin{cases} \frac{d}{dt}w_1(t) \\ \quad = -(d_m+2D_m)w_1(t) + D_m(w_2(t)+w_3(t)) \\ \qquad + \frac{1}{3}\rho(1+2r^*)b(w_1(t-r)) \\ \qquad + \frac{1}{3}\rho(1-r^*)(b(w_2(t-r))+b(w_3(t-r))) \\ \frac{d}{dt}w_2(t) \\ \quad = -(d_m+2D_m)w_2(t) + D_m(w_1(t)+w_3(t)) \\ \qquad + \frac{1}{3}\rho(1+2r^*)b(w_2(t-r)) \\ \qquad + \frac{1}{3}\rho(1-r^*)(b(w_1(t-r))+b(w_3(t-r))) \\ \frac{d}{dt}w_3(t) \\ \quad = -(d_m+2D_m)w_3(t) + D_m(w_1(t)+w_2(t)) \\ \qquad + \frac{1}{3}\rho(1+2r^*)b(w_3(t-r)) \\ \qquad + \frac{1}{3}\rho(1-r^*)(b(w_1(t-r))+b(w_2(t-r))). \end{cases} \tag{3.1}$$

The equilibria for the above system satisfy

$$\begin{cases} -(d_m+2D_m)w_1 + D_m(w_2+w_3) \\ \quad +\frac{1}{3}\rho(1+2r^*)b(w_1) \\ \quad +\frac{1}{3}\rho(1-r^*)[b(w_2)+b(w_3)] = 0, \\ -(d_m+2D_m)w_2 + D_m(w_1+w_3) \\ \quad +\frac{1}{3}\rho(1+2r^*)b(w_2) \\ \quad +\frac{1}{3}\rho(1-r^*)[b(w_1)+b(w_3)] = 0, \\ -(d_m+2D_m)w_3 + D_m(w_1+w_2) \\ \quad +\frac{1}{3}\rho(1+2r^*)b(w_3) \\ \quad +\frac{1}{3}\rho(1-r^*)[b(w_1)+b(w_2)] = 0. \end{cases} \tag{3.2}$$

Since (3.2) is symmetric for w_1, w_2, w_3, it is reasonable to concentrate on the existence of homogeneous equilibria, that is, equilibria of the form

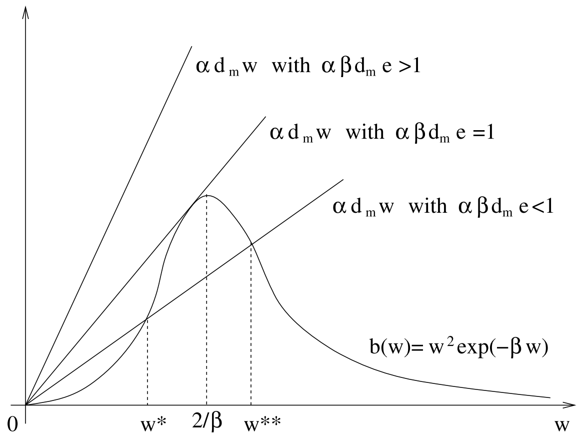

Fig. 1 The structure of solutions of (3.3)

$E(w_1, w_2, w_3)$ with $w_1 = w_2 = w_3 =: w$. Obviously, homogeneous equilibria of (3.2) are totally determined by the scalar equation

$$d_m w = \rho b(w). \tag{3.3}$$

For convenience, we denote $\alpha := e^{\int_0^r d_I(a)da} = \frac{1}{\rho}$, and as in [10], we choose a particular birth function

$$b(w) = w^2 e^{-\beta w}, \quad \beta > 0. \tag{3.4}$$

This birth function corresponds to a one-hump per capita birth rate $we^{-\beta w}$ which may account for the Allee Effect in population biology. For this birth function, note that $w = 0$ is always a solution. For other possible positive solutions, it is easy to obtain the following conclusions (see Fig. 1 for a demonstration):

(i) If $\alpha > \frac{1}{\beta d_m e}$, then (3.3) has no positive solutions.
(ii) If $\alpha = \frac{1}{\beta d_m e}$, then (3.3) has exactly one positive solution.
(iii) If $\alpha < \frac{1}{\beta d_m e}$, (3.3) has exactly two positive solutions.

In order to study the stability of a homogeneous equilibrium $(\bar{w}, \bar{w}, \bar{w})$ of (3.1), we need to consider the characteristic equation of (3.1) at the equilibrium:

$$\begin{vmatrix} \lambda + s_1 & -s_2 & -s_2 \\ -s_2 & \lambda + s_1 & -s_2 \\ -s_2 & -s_2 & \lambda + s_1 \end{vmatrix} = 0, \tag{3.5}$$

where

$$s_1 = s_1(\lambda) := d_m + 2D_m - \frac{1}{3}\rho(1+2r^*)b'(\bar{w})e^{-\lambda r}$$

and

$$s_2 = s_2(\lambda) := D_m + \frac{1}{3}\rho(1-r^*)b'(\bar{w})e^{-\lambda r}.$$

Simple calculation shows that (3.5) is equivalent to

$$(\lambda + s_1 - 2s_2)(\lambda + s_1 + s_2)^2 = 0. \tag{3.6}$$

At the trivial equilibrium $E_0 = E(0,0,0)$, $b'(0) = 0$ gives $s_1 = d_m + 2D_m$ and $s_2 = D_m$, and thus, the corresponding characteristic equation becomes

$$(\lambda + d_m)(\lambda + d_m + 3D_m)^2 = 0,$$

whose eigenvalues are all negative. Therefore, E_0 is always asymptotically stable.

From now on, we will assume the condition

$$\alpha < \frac{1}{\beta d_m e} \tag{3.7}$$

so that (3.1) has, in addition to the trivial equilibrium E_0, two positive homogeneous equilibria denoted by $E^* = (w^*, w^*, w^*)$ and $E^{**} = (w^{**}, w^{**}, w^{**})$, satisfying

$$0 < w^* < 1/\beta < w^{**} \quad \text{and} \quad d_m < \rho b'(w^*). \tag{3.8}$$

Furthermore, since

$$\begin{aligned}
&b'(w) = we^{-\beta w}(2 - \beta w),\\
&b''(w) = e^{-\beta w}\big(2 - 4\beta w + \beta^2 w^2\big),\\
&b'\left(\frac{1}{\beta}\right) = \frac{1}{\beta e}, \qquad b'\left(\frac{2}{\beta}\right) = 0, \qquad b'(\infty) = 0,\\
&b''(w) < 0, \quad \forall w \in \left(\frac{1}{\beta}, \frac{2}{\beta}\right],
\end{aligned}$$

we conclude that

$$\begin{aligned}
&0 < b'(w^{**}) < \frac{1}{\beta e} \quad \text{if } w^{**} \in \left(\frac{1}{\beta}, \frac{2}{\beta}\right), \quad \text{and}\\
&b'(w^{**}) < 0 \quad \text{if } w^{**} \in \left(\frac{2}{\beta}, \infty\right).
\end{aligned} \tag{3.9}$$

In the sequel, we analyze the stability of these two positive homogeneous equilibria. Note that λ satisfies (3.6) if and only if

$$\begin{aligned}
&\lambda + s_1 - 2s_2 = 0, \quad \text{i.e.}\\
&\lambda + d_m - \rho b'(\bar{w})e^{-\lambda r} = 0,
\end{aligned} \tag{3.10}$$

or

$$\begin{aligned}
&\lambda + s_1 + s_2 = 0, \quad \text{i.e.}\\
&\lambda + d_m + 3D_m - \rho r^* b'(\bar{w})e^{-\lambda r} = 0.
\end{aligned} \tag{3.11}$$

For E^*, by (3.8) and the well-known results on Hayes equation (see, e.g., Theorem A.5 in [5]), it follows that E^* is always unstable.

For the stability of the largest equilibrium E^{**}, we distinguish three cases:

- Case 1: $w^{**} \in (1\beta, 2/\beta)$.
- Case 2: $w^{**} = 2/\beta$.
- Case 3: $w^{**} \in (2/\beta, \infty)$.

For Case 2 , $b'(w^{**}) = 0$, and hence (3.10) and (3.11) become $\lambda + d_m = 0$ and $\lambda + d_m + 3D_m = 0$ respectively. Obviously E^{**} is asymptotic stable in this case, since all roots of these two equations are real and negative. Thus, in the rest of this section, we only need to consider the Cases 1 and 3.

Firstly we note that E^{**} is stable when α is large (or equivalently ρ is small, merely for mathematical purposes), since roots of (3.10) and (3.11) are negative real numbers when $\rho \to 0$). E^{**} may lose its stability as α decreases to lower level, and this can happen through the occurrence of pure imaginary roots of the corresponding characteristic equation.

We first consider Case 3, implying $b'(w^{**}) < 0$. Substituting $\lambda = i\omega, \omega > 0$ into (3.10) and (3.11) and separating the real parts from the purely imaginary parts lead respectively to

$$d_m = \rho b'(w^{**})\cos(\omega r), \quad \omega = -\rho b'(w^{**})\sin(\omega r), \tag{3.12}$$

$$\begin{aligned}
&d_m + 3D_m = \rho r^* b'(w^{**})\cos(\omega r),\\
&\quad \omega = -\rho r^* b'(w^{**})\sin(\omega r).
\end{aligned} \tag{3.13}$$

The negativity of $b'(w^{**})$ implies that ωr is in the second quadrant. Denote by $\theta = \theta(u)$ the unique solution of

$$\frac{-\theta}{ur} = \tan\theta, \quad \theta \in \left(\frac{\pi}{2}, \pi\right). \tag{3.14}$$

Let

$$\begin{aligned}
\alpha_1 &= \frac{-b'(w^{**})}{\sqrt{d_m^2 + \left[\frac{\theta(d_m)}{r}\right]^2}},\\
\alpha_2 &= \frac{-r^* b'(w^{**})}{\sqrt{(d_m + 3D_m)^2 + \left[\frac{\theta(d_m + 3D_m)}{r}\right]^2}}.
\end{aligned} \tag{3.15}$$

Then α_1 (α_2) is the first α value from the above for which (3.12) (or (3.13)) has a pair of purely imaginary roots $\pm i\omega_1(\pm i\omega_2)$, where

$$\begin{aligned} \omega_1 &= \sqrt{\left[\frac{b'(w^{**})}{\alpha_1}\right]^2 - d_m^2}, \\ \omega_2 &= \sqrt{\left[\frac{r^* b'(w^{**})}{\alpha_2}\right]^2 - (d_m + 3D_m)^2}. \end{aligned} \tag{3.16}$$

It is easily seen that $\theta(u)$ is increasing in u and hence, $0 < \alpha_2 < \alpha_1$.

Due to the assumption (3.7), we would like to compare α_1 with $\frac{1}{\beta d_m e}$. Noticing that

$$\min_{w\in(\frac{1}{\beta},\infty)} \{b'(w)\} = -\frac{2+2\sqrt{2}}{\beta} e^{-(2+\sqrt{2})},$$

and using the inequality

$$\begin{aligned} e^{2+\sqrt{2}} &= e \cdot e^{1+\sqrt{2}} \\ &= e\left[1 + \left(1+\sqrt{2}\right) + \frac{(1+\sqrt{2})^2}{2} + \cdots\right] \\ &> e\left(2+2\sqrt{2}\right), \end{aligned}$$

we obtain

$$\begin{aligned} \alpha_1 &\le \frac{2+2\sqrt{2}}{\beta\sqrt{d_m^2 + [\frac{\theta(d_m)}{r}]^2}} e^{-(2+\sqrt{2})} \\ &< \frac{2+2\sqrt{2}}{\beta d_m} e^{-(2+\sqrt{2})} < \frac{1}{\beta d_m e}. \end{aligned}$$

From the above, we conclude that when $\frac{1}{\beta d_m e} > \alpha > \alpha_1$, all roots of (3.10) and (3.11) have negative real parts and thus, E^{**} is asymptotically stable.

When $\alpha = \alpha_1$, then all roots of (3.11) have negative real parts, and (3.10) has a pair of purely imaginary roots $\pm i\omega_1$ satisfying the following transversality condition:

$$\left.\frac{d\,\mathrm{Re}(\lambda)}{d\alpha}\right|_{\alpha=\alpha_1} = -\frac{\alpha_1^2 d_m + r[b'(w^{**})]^2}{\alpha_1^3 + 2\alpha_1^3 r d_m + \alpha_1[r b'(w^{**})]^2} < 0. \tag{3.17}$$

Therefore, Hopf bifurcation occurs from the equilibrium E^{**} at $\alpha = \alpha_1$ (see [6]). The bifurcated periodic solutions are synchronized because the synchronized solutions of (3.1) are described by the scalar equation

$$\frac{dw(t)}{dt} = -d_m w(t) + \rho b\big(w(t-r)\big)$$

which has (3.10) as its characteristic equation at the positive equilibrium $w = w^{**}$, and hence has a Hopf bifurcation at $\alpha = \alpha_1$ as well.

When $\alpha \in (\alpha_2, \alpha_1)$, all roots of (3.11) have negative real parts, and (3.10) has a pair of conjugate complex roots with positive real parts. Thus E^{**} is unstable.

When $\alpha = \alpha_2$, (3.10) has a pair of conjugate complex roots with positive real parts, and (3.11) has a pair of purely imaginary roots $\pm i\omega_2$ satisfying the following transversality condition:

$$\begin{aligned} &\left.\frac{d\,\mathrm{Re}(\lambda)}{d\alpha}\right|_{\alpha=\alpha_2} \\ &\quad = -\frac{\alpha_2^2(d_m + 3D_m) + r[r^* b'(w^{**})]^2}{\alpha_2^3 + 2\alpha_2^3 r(d_m + 3D_m) + \alpha_2[r r^* b'(w^{**})]^2} \\ &\quad < 0. \end{aligned}$$

Notice that the multiplicity of $\pm i\omega_2$ is 2 (see (3.6)), and thus, the classic Hopf bifurcation theorem (see [6]) cannot be applied. However, (3.1) is a symmetric system, and therefore, we can apply a Hopf bifurcation theorem for symmetric functional differential equations (e.g., Theorem 2.1 in [12]) to explore symmetric Hopf bifurcations near E^{**} which may lead to the existence of phase-locked periodic solutions, mirror-reflecting waves and standing waves, as stated in the following theorem.

Theorem 3.1 *Assume that $\alpha < \frac{1}{\beta d_m e}$, and $w^{**} \in (\frac{2}{\beta}, \infty)$. Let α_1 and α_2 be defined as in (3.15).*

(i) *E^{**} is asymptotically stable if $\frac{1}{\beta d_m e} > \alpha > \alpha_1$, and unstable when $\alpha < \alpha_1$.*
(ii) *When α decreases to pass α_1, (3.1) experiences a Hopf bifurcation from E^{**}, giving rise to a synchronous periodic solution with period T near $2\pi/\omega_1$, where ω_1 is defined in (3.16).*
(iii) *When α further decreases to pass α_2, (3.1) experiences a symmetric Hopf bifurcation from E^{**}, giving rise to eight branches of asynchronous periodic solutions with period T near $2\pi/\omega_2$ (where ω_2 is defined in (3.6)), and these branches are:*

(iii-1) *two phase-locked periodic solutions satisfying* $w_j(t) = w_{j-1}(t \pm \frac{T}{3})$, $j \pmod 3$, $t \in \mathcal{R}$;

(iii-2) *three mirror-reflecting waves satisfying* $w_i(t) = w_j(t) \neq w_k(t)$ *for* $t \in \mathcal{R}$ *and distinct* $i, j, k \in \{1, 2, 3\}$;

(iii-3) *three standing waves satisfying* $w_i(t) = w_j(t + \frac{T}{2})$ *for* $t \in \mathcal{R}$, $i, j \in \{1, 2, 3\}$ *and* $i \neq j$.

Proof We have already shown the conclusions (i)–(ii) before the theorem. The proof of conclusion (iii) can be completed by applying Theorem 2.1 in [12]. To this end, we need to verify all conditions of Theorem 2.1 in [12] for the model (2.18). Such verification work is similar to those in [1, 3, 4, 15] for some neural network models with a ring structure, for readers' convenience, we give the details below.

Let $\mathcal{D}_3$ be the dihedral group of order 6, and define the action of $\mathcal{D}_3$ on $\mathcal{R}^3 = \{w : w = (w_1, w_2, w_3)\}$ by

$$(\gamma w)_j = w_{j-1}, \qquad (\kappa w)_j = w_{3-j}, \quad j \pmod 3,$$

where γ is the generator of the cyclic group $\mathcal{Z}_3$, and κ represents the flip action. Then it is easy to show that the right side of the system (3.1) is $\mathcal{D}_3$-equivariant (see [12] for the definition of $\mathcal{D}_3$-equivariant), and thus the assumption (H_2) in [12] is satisfied.

Next, let

$$\xi = e^{i\frac{2\pi}{3}}, \qquad v_j = \left(1, \xi^j, \xi^{2j}\right), \quad j = 1, 2,$$

$$\Delta(\alpha_2, i\omega_2) = \begin{pmatrix} \lambda + s_1 & -s_2 & -s_2 \\ -s_2 & \lambda + s_1 & -s_2 \\ -s_2 & -s_2 & \lambda + s_1 \end{pmatrix}\Bigg|_{\substack{\alpha=\alpha_2 \\ \lambda=i\omega_2}},$$

where s_1, s_2 are as in (3.6) with $\bar{w} = w^{**}$. Then we have

$$v_j^{\mathrm{T}} v_i = 3 \quad \text{as } i, j \in \{1, 2\},\ i \neq j,$$
$$v_j^{\mathrm{T}} v_j = 0 \quad \text{as } j \in \{1, 2\}, \quad v_1 = \bar{v}_2,$$
$$1 + \xi^j + \xi^{2j} = 0, \quad j = 1, 2.$$

Noting that $\lambda + s_1 + s_2 = 0$ when $\alpha = \alpha_2$ and $\lambda = i\omega_2$, we obtain

$$\operatorname{Ker} \Delta(\alpha_2, i\omega_2) = \operatorname{span}\{v_1, v_2\},$$
$$\dim \operatorname{Ker} \Delta(\alpha_2, i\omega_2) = 4,$$

and we conclude that there exists a 2-dimensional absolutely irreducible representation $\mathcal{R}^2$ of $\mathcal{D}_3$ such that $\operatorname{Ker} \Delta(\alpha_2, i\omega_2)$ is $\mathcal{D}_3$-isomorphic to $\mathcal{R}^2 \oplus \mathcal{R}^2$. Therefore, the assumption (H_3) in [12] is also satisfied.

Thirdly, the generalized eigenspace corresponding to $\pm i\omega_2$ consists of $\operatorname{Re}(e^{i\omega_2} v)$ and $\operatorname{Im}(e^{i\omega_2} v)$, where $v \in \operatorname{Ker} \Delta(\alpha_2, i\omega_2)$. Therefore, the assumption (H_1) in [12] is satisfied as well.

The above and (3.12) verify all the conditions of Theorem 2.1 in [12] for system (3.1) at E^{**}. By this theorem, we conclude that when α decreases to pass α_2, there are various periodic solutions bifurcated from E^{**}. In order to apply Theorem 2.1 in [12] to obtain the results in (iv-1)–(iv-3), we need to explore the symmetries of these bifurcated periodic solutions. To this end, we need some preparation.

Let $\tau = \frac{2\pi}{\omega_2}$ and $S^1 = \{z : |z| = 1, z \in \mathcal{C}\}$. Denote by P_τ the Banach space of all continuous τ-periodic mappings $w : \mathcal{R} \to \mathcal{R}^3$ with the supremum norm, and let SP_τ be the subspace of P_τ consisting of all τ-periodic solutions of the linearization of (3.1) at $w = w^{**}$ with $\alpha = \alpha_2$. Then,

$$SP_\tau = \left\{ \sum_{i=1}^{4} x_i \epsilon_i : x_i \in \mathcal{R},\ i = 1, 2, 3, 4 \right\},$$

where

$$\epsilon_1 = \cos\left(\frac{2\pi}{\tau} t\right) \operatorname{Re} v_1 - \sin\left(\frac{2\pi}{\tau} t\right) \operatorname{Im} v_1,$$

$$\epsilon_2 = \sin\left(\frac{2\pi}{\tau} t\right) \operatorname{Re} v_1 + \cos\left(\frac{2\pi}{\tau} t\right) \operatorname{Im} v_1,$$

$$\epsilon_3 = \cos\left(\frac{2\pi}{\tau} t\right) \operatorname{Re} v_1 + \sin\left(\frac{2\pi}{\tau} t\right) \operatorname{Im} v_1,$$

$$\epsilon_4 = \sin\left(\frac{2\pi}{\tau} t\right) \operatorname{Re} v_1 - \cos\left(\frac{2\pi}{\tau} t\right) \operatorname{Im} v_1.$$

Let $\mathcal{D}_3 \times S^1$ act on P_τ by

$$(\chi, \theta) w = \chi w(t + \theta), \quad (\chi, \theta) \in \mathcal{D}_3 \times S^1,\ w \in P_\tau.$$

Then, SP_τ is a $\mathcal{D}_3 \times S^1$-invariant subspace of P_T. In the rest of the proof, we need to identify all subgroups of $\mathcal{D}_3 \times S^1$ satisfying the conditions of Theorem 2.1 in [12], by which we can obtain (iii-1)–(iii-3).

Proof of (iii-1) For $\theta \in (0, \tau)$, let

$$\Sigma_\theta = \left\{ \left(\gamma^j, e^{i\omega_2 j\theta}\right) : j = 0, 1, 2 \right\}.$$

Then Σ_θ is a subgroup of $\mathcal{D}_3 \times S^1$. Consider the fixed points set in SP_τ under the action of this subgroup:

$$\begin{aligned}\mathrm{Fix}(\Sigma_\theta, SP_\tau)\\ &= \{w \in SP_\tau : (\chi,\theta)w = w, (\chi,\theta)\in\Sigma_\theta\}\\ &= \{w \in SP_\tau : \gamma w(t) = w(t-\theta), t \in \mathcal{R}\}\\ &= \{w \in SP_\tau : w_{j-1}(t) = w_j(t-\theta),\\ &\quad j \pmod 3,\ t\in\mathcal{R}\}.\end{aligned}$$

It is easily seen that

$$\gamma\sum_{i=1}^4 x_i\epsilon_i = \left(\sum_{i=1}^4 x_i\epsilon_i\right)(\cdot-\theta)$$

if and only if

$$\begin{aligned}&x_3 = x_4 = 0, && x_1, x_2 \in \mathcal{R}, && \text{as } \theta = \frac{2\tau}{3},\\ &x_1 = x_2 = 0, && x_3, x_4\in\mathcal{R}, && \text{as } \theta = \frac{\tau}{3},\\ &x_1 = x_2 = x_3 = x_4 = 0, && && \text{as } \theta \neq \frac{\tau}{3}, \frac{2\tau}{3}.\end{aligned}$$

Therefore,

$$\mathrm{Fix}(\Sigma_\theta, SP_\tau) = \begin{cases}\{x_1\epsilon_1 + x_2\epsilon_2 : x_1, x_2\in\mathcal{R}\}, & \text{as } \theta = \frac{\tau}{3},\\ \{x_3\epsilon_3 + x_4\epsilon_4 : x_3, x_4\in\mathcal{R}\}, & \text{as } \theta = \frac{2\tau}{3},\\ \{0\} & \text{as } \theta \neq \frac{\tau}{3}, \frac{2\tau}{3}.\end{cases}$$

Hence, $\dim(\mathrm{Fix}(\Sigma_\theta, SP_\tau)) = 2$ for two values of $\theta \in (0,\tau)$, that is, $\theta = \frac{\tau}{3}$ or $\frac{2\tau}{3}$. In view of the conclusion of Theorem 2.1 in [12], the subgroup Σ_θ at $\theta = \frac{\tau}{3}$ accounts for a phase-locked periodic solution of (3.1) satisfying $w_j(t) = w_{j-1}(t+\frac{T}{3})$, $j \pmod 3$, while the subgroup Σ_θ at $\theta = \frac{2\tau}{3}$ is responsible for a phase-locked periodic solution of (3.1) satisfying $w_j(t) = w_{j-1}(t-\frac{T}{3})$, $j \pmod 3$ for $t\in\mathcal{R}$, where the period T is near $\tau = \frac{2\pi}{\omega_2}$. This completes the proof of (iii-1). □

Proof of (iii-2) Denote $\Sigma_m = \{(\kappa,1),(1,1)\}$, then Σ_m is a subgroup of $\mathcal{D}_3\times S^1$, and the fixed points set in SP_τ under this subgroup is:

$$\begin{aligned}\mathrm{Fix}(\Sigma_m, SP_\tau)\\ &= \{w\in SP_\tau : (\chi,\theta)w = w, (\chi,\theta)\in\Sigma_m\}\\ &= \{w\in SP_\tau : \kappa w(t) = w(t), t\in\mathcal{R}\}\\ &= \{w\in SP_\tau : w_{3-j}(t) = w_j(t), j \pmod 3,\ t\in\mathcal{R}\}.\end{aligned}$$

Note that

$$\begin{aligned}\kappa(x_1\epsilon_1 + x_2\epsilon_2 + x_3\epsilon_3 + x_4\epsilon_4)\\ = x_1\epsilon_1 + x_2\epsilon_2 + x_3\epsilon_3 + x_4\epsilon_4\end{aligned}$$

if and only if

$$\begin{aligned}&x_3 = x_1\cos\left(\frac{4\pi}{3}\right) - x_2\sin\left(\frac{4\pi}{3}\right),\\ &x_4 = x_1\sin\left(\frac{4\pi}{3}\right) + x_2\cos\left(\frac{4\pi}{3}\right), \quad x_1, x_2\in\mathcal{R}.\end{aligned}$$

Therefore

$$\begin{aligned}\mathrm{Fix}(\Sigma_m, SP_\tau)\\ &= \left\{\sum_{i=1}^4 x_i\epsilon_i : x_3 = x_1\cos\left(\frac{4\pi}{3}\right) - x_2\sin\left(\frac{4\pi}{3}\right),\right.\\ &\qquad \left. x_4 = x_1\sin\left(\frac{4\pi}{3}\right) + x_2\cos\left(\frac{4\pi}{3}\right),\ x_1, x_2\in\mathcal{R}\right\},\end{aligned}$$

which implies $\dim\mathrm{Fix}(\Sigma_m, SP_\tau) = 2$. In view of the conclusion of Theorem 2.1 in [12], there exist 3 mirror-reflecting waves of (3.1) satisfying $w_i(t) = w_j(t) \neq w_k(t)$ for $t\in\mathcal{R}$, $(i,j,k)\in\{1,2,3\}$, where i, j, k are distinct, completing the proof of (iii-2). □

Proof of (iii-3) Denote $\Sigma_s = \{(\kappa,-1),(1,1)\}$, then Σ_s is a subgroup of $\mathcal{D}_3\times S^1$. If $\theta\in\{0,\frac{\tau}{2}\}$ where $\tau = \frac{2\pi}{\omega_2}$, then

$$e^{i\omega_2\theta} = \begin{cases}1, & \theta = 0,\\ -1, & \theta = \frac{\tau}{2}.\end{cases}$$

Note that

$$\begin{aligned}\mathrm{Fix}(\Sigma_s, SP_\tau)\\ &= \{w\in SP_\tau : (\chi,\theta)w = w,\ (\chi,\theta)\in\Sigma_s\}\\ &= \left\{w\in SP_\tau : \kappa w(t) = w\left(t+\frac{\tau}{2}\right),\ t\in\mathcal{R}\right\}\\ &= \left\{w\in SP_\tau : w_{3-j}(t) = w_j\left(t+\frac{\tau}{2}\right),\right.\\ &\qquad \left. j \pmod 3,\ t\in\mathcal{R}\right\}\\ &= \left\{\sum_{i=1}^4 x_i\epsilon_i : x_3 = -x_1\cos\left(\frac{4\pi}{3}\right) + x_2\sin\left(\frac{4\pi}{3}\right),\right.\\ &\qquad \left. x_4 = -x_1\sin\left(\frac{4\pi}{3}\right) - x_2\cos\left(\frac{4\pi}{3}\right),\ x_1, x_2\in\mathcal{R}\right\}\end{aligned}$$

and thus,

$\dim \mathrm{Fix}(\Sigma_s, SP_\tau) = 2.$

Again by Theorem 2.1 in [12], there exist 3 standing waves satisfying $w_i(t) = w_j(t + \frac{T_\omega}{2})$ for $t \in \mathcal{R}$, $(i, j) \in \{1, 2, 3\}$ and $i \neq j$, where T_ω is near $\tau = \frac{2\pi}{\omega_2}$. This completes the proof of (iii-3) and hence the proof of Theorem 3.1. □

Finally, we consider the remaining *Case* 1: $w^{**} \in (\frac{1}{\beta}, \frac{2}{\beta})$, which implies $\frac{1}{\beta e} > b'(w^{**}) > 0$ (see (3.9)). Again, we need to solve (3.12) and (3.13) for $\omega > 0$. Now the positivity of $b'(w^{**})$ implies that $\omega r \in (3\pi/2, 2\pi)$, and thus, we need to replace (3.14) by

$$\frac{-\bar{\theta}}{ur} = \tan\bar{\theta}, \quad \bar{\theta} \in \left(\frac{3\pi}{2}, 2\pi\right). \tag{3.18}$$

Denote by $\bar{\theta} = \bar{\theta}(u)$ the unique solution of (3.18), and let

$$\begin{aligned} \bar{\alpha}_1 &= \frac{b'(w^{**})}{\sqrt{d_m^2 + \left[\frac{\bar{\theta}(d_m)}{r}\right]^2}}, \\ \bar{\alpha}_2 &= \frac{r^* b'(w^{**})}{\sqrt{(d_m + 3D_m)^2 + \left[\frac{\bar{\theta}(d_m+3D_m)}{r}\right]^2}}. \end{aligned} \tag{3.19}$$

Then $\bar{\alpha}_1$ ($\bar{\alpha}_2$) is the first α value from the above for which (3.12) (or (3.13)) has a pair of purely imaginary roots $\pm\omega_1(\pm i\omega_2)$, where

$$\begin{aligned} \bar{\omega}_1 &= \sqrt{\left[\frac{b'(w^{**})}{\bar{\alpha}_1}\right]^2 - d_m^2}, \\ \bar{\omega}_2 &= \sqrt{\left[\frac{r^* b'(w^{**})}{\bar{\alpha}_2}\right]^2 - (d_m + 3D_m)^2}. \end{aligned} \tag{3.20}$$

We can also easily verify the transversality condition

$$\left.\frac{d\,\mathrm{Re}(\lambda)}{d\alpha}\right|_{\alpha=\bar{\alpha}_i} < 0, \quad i = 1, 2.$$

Therefore, repeating the proof of Theorem 3.1, one can conclude that when α decreases to pass the critical value $\bar{\alpha}_1$ and then $\bar{\alpha}_2$, there occur Hopf bifurcations with the same symmetries described in Theorem 3.1.

However, there is a difference between Case 1 and Case 3: in Case 3, E^{**} remains stable for $\alpha \in (\alpha_1, 1/\beta d_m e)$ and when α passes α_1, E^{**} loses its stability to some periodic solutions due to Hopf bifurcations; while in Case 1, E^{**} has already lost its stability before $\bar{\alpha}_1$. Indeed, the condition $b'(w^{**}) > 0$ allows (3.10) to have the zero root $\lambda = 0$ at

$$\alpha = \bar{\alpha}_{0,1} := \frac{b'(w^{**})}{d_m}, \tag{3.21}$$

and also allows (3.11) to have the zero root at

$$\alpha = \bar{\alpha}_{0,2} := \frac{r^* b'(w^{**})}{d_m + 3D_m}. \tag{3.22}$$

Obviously, these critical values have the following relations:

$$\bar{\alpha}_2 < \bar{\alpha}_1 < \bar{\alpha}_{0,1}, \qquad \bar{\alpha}_2 < \bar{\alpha}_{0,2} < \bar{\alpha}_{0,1}. \tag{3.23}$$

One can also verify the transversality condition at $\alpha = \bar{\alpha}_{0,1}$ and $\alpha = \bar{\alpha}_{0,2}$ for (3.10). Thus, E^{**} already becomes unstable when $\alpha \in (\alpha_1, \alpha_{0,1})$, before Hopf bifurcations occur at $\alpha = \alpha_1$ and $\alpha = \alpha_2$.

Summarizing the above, we have the following theorem for Case 1.

Theorem 3.2 *Assume that* $\alpha < \frac{1}{\beta d_m e}$, *and* $w^{**} \in (\frac{1}{\beta}, \frac{2}{\beta})$. *Let* $\bar{\alpha}_1$, $\bar{\alpha}_2$, $\bar{\alpha}_{0,1}$ *and* $\bar{\alpha}_{0,2}$ *be defined in* (3.19), (3.21) *and* (3.22) *respectively*:

(i) E^{**} *is asymptotically stable if* $\frac{1}{\beta d_m e} > \alpha > \bar{\alpha}_{0,1}$, *and unstable when* $\alpha < \bar{\alpha}_{0,1}$.

(ii) *When* α *decreases to pass* $\bar{\alpha}_1$, (3.1) *experiences a Hopf bifurcation from* E^{**} *giving rise to a synchronous periodic solution with period* T *near* $2\pi/\bar{\omega}_1$, *where* $\bar{\omega}_1$ *is defined in* (3.20).

(iii) *When* α *decreases to pass* $\bar{\alpha}_2$, (3.1) *experiences a symmetric Hopf bifurcation from* E^{**}, *giving rise to eight branches of asynchronous periodic solutions with period* T *near* $2\pi/\bar{\omega}_2$ *(where* $\bar{\omega}_2$ *is defined in* (3.20)), *and these branches are*:

  (iii-1) *two phase-locked periodic solutions satisfying* $w_j(t) = w_{j-1}(t \pm \frac{T}{3})$, $j \pmod 3$, $t \in \mathcal{R}$;

  (iii-2) *three mirror-reflecting waves satisfying* $w_i(t) = w_j(t) \neq w_k(t)$ *for* $t \in \mathcal{R}$ *and distinct* $i, j, k \in \{1, 2, 3\}$;

  (iii-3) *three standing waves satisfying* $w_i(t) = w_j(t + \frac{T}{2})$ *for* $t \in \mathcal{R}$, $i, j \in \{1, 2, 3\}$ *and* $i \neq j$.

Remark 3.1 In Case 1, the equilibrium E^{**} loses its stability when α decreases to pass $\alpha = \bar{\alpha}_{0,1}$ at which the characteristic equation has a zero eigenvalue while

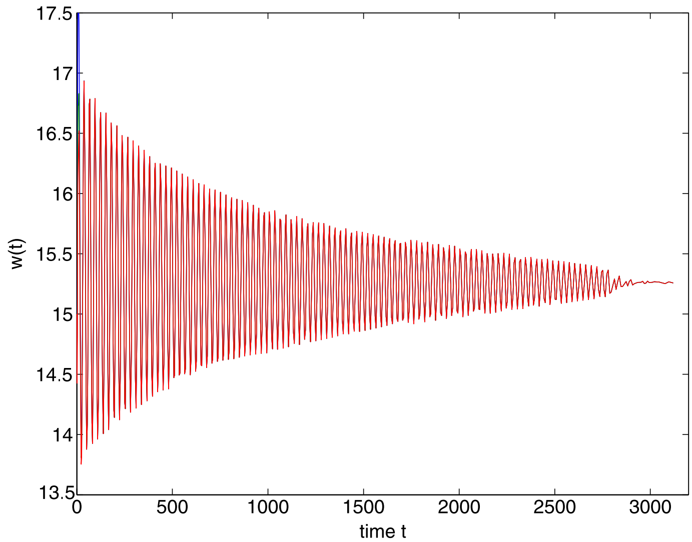

Fig. 2 Transient oscillation of solutions of (3.1). Here $d_m = 0.07$, $D_m = 0.01$, $r = 8.5$, $r^* = 0.1$, $\beta = \frac{1}{2}\ln 2$, $\alpha = 1.1 > \alpha_1 \approx 1.092983$, $w^{**} = 15.2617$ and the initial conditions are $(w_1(t), w_2(t), w_3(t)) = (1.8t + 15, 15, -1.8t + 15)$, $t \in [-r, 0]$. The *three curves* in the figure represent $w_1(t), w_2(t), w_3(t)$ respectively

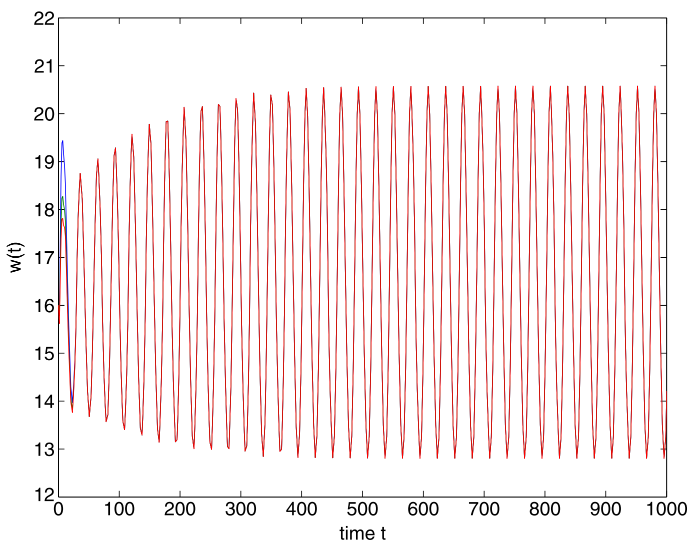

Fig. 3 Synchronous periodic solutions of (3.1). Here $d_m = 0.07$, $D_m = 0.01$, $r = 8.5$, $r^* = 0.1$, $\beta = \frac{1}{2}\ln 2$, $\alpha = 0.9$, $w^{**} = 15.9719$ and the initial conditions are $(w_1(t), w_2(t), w_3(t)) = (1.88t + 16, 16, -1.88t + 16)$, $t \in [-r, 0]$. The *three curves* in the figure represent $w_1(t), w_2(t), w_3(t)$ respectively, giving a synchronized periodic solution

all other eigenvalues have negative real parts. Thus, bifurcation at this value is interesting and important to this model. At another smaller critical value $\bar{\alpha}_{0,2}$, the characteristic equation also has a zero eigenvalue. It would also be interesting to know what happens when α pass this value. There may be equilibrium bifurcation at these values giving rise to non-homogeneous positive equilibria carrying certain symmetries. We choose not to discuss these two values in detail in this already lengthy paper, and will instead leave it as a future work.

Remark 3.2 For Case 3, the equilibrium E^{**} loses its stability when α decreases to pass $\alpha = \alpha_1$, yielding to a branch of synchronous periodic solutions. Among those periodic solutions stated in Theorem 3.1, only this branch can possibly be stable since for those asynchronous ones, there is at least one eigenvalue that has positive real part. Since the pair of purely imaginary roots at α_1 are simple, the standard algorithms developed in Hassard et al. [6] can be applied to determine the direction and stability of the bifurcated synchronous periodic solutions. Due to the limitation of space, we choose not to give the straightforward but tedious computations here for the formulas that determine the bifurcation direction and stability. Our numeric simulations seem to suggest that the bifurcation at α_1 is supercritical and the bifurcated synchronous periodic solution is stable. See Fig. 3 for an illustration. Also in this case, since the right most pair of eigenvalues cross the purely imaginary axis in the complex plane via a pair of non-zero eigenvalues as α passes α_1, transient oscillations should occur when α is in the right neighborhood of α_1, and this is confirmed by simulations as shown in Fig. 2.

References

1. Campbell, S.A., Yuan, Y., Bungay, S.D.: Equivariant Hopf bifurcation in a ring of identical cells with delayed coupling. Nonlinearity **18**, 2827–2846 (2005)
2. Campbell, S.A., Ncube, I., Wu, J.: Multistability and stable asynchronous periodic oscillations in a multiple-delayed neural system. Physica D **214**, 101–119 (2006)
3. Guo, S.: Spatiotemporal patterns of nonlinear oscillations in an excitatory ring network with delay. Nonlinearity **18**, 2391–2407 (2005)
4. Guo, S., Huang, L.: Hopf bifurcating periodic orbits in a ring of neurons with delays. Physica D **183**, 19–44 (2003)
5. Hale, J.K., Verduyn Lunel, S.M.: Introduction to Functional Differential Equations. Applied Mathematical Sciences, vol. 99. Springer, New York (1993)
6. Hassard, B., Kazarinoff, N., Wan, Y.H.: Theory and Applications of Hopf Bifurcation. London Mathematical Society Lecture Notes Series, vol. 41. Cambridge Univ. Press, Cambridge (1981)
7. He, X.-Z., Wu, J., Zou, X.: Dynamics of single species populations over a patchy environment. In: Chen, L., Ruan, S., Zhu, J. (eds.) Advanced Topics in Biomathematics, pp. 63–77. World Scientific, Singapore (1998)
8. Madras, N., Wu, J., Zou, X.: Local–nonlocal interaction and spatiotemporal patterns in single-species population over a patch environment. Can. Appl. Math. Q. **4**, 109–134 (1996)
9. Metz, J.A.J., Dielmann, O.: The Dynamics of Physiologically Structured Populations. Springer, Berlin (1986)
10. So, J.W.-H., Wu, J., Zou, X.: Structured population on two patches: modeling dispersal and delay. J. Math. Biol. **43**, 37–51 (2001)
11. Wei, J.J., Yuan, Y.: Synchronized Hopf bifurcation analysis in a neural network model with delays. J. Math. Anal. Appl. **312**, 205–229 (2005)
12. Wu, J.: Symmetric functional differential equations and neural networks with memory. Trans. Am. Math. Soc. **350**, 4799–4838 (1998)
13. Wu, J.: Synchronization and stable phase-locking in a network of neurons with memory. Math. Comput. Model. **30**, 117–138 (1999)
14. Wu, J., Krawcewicz, W.: Discrete waves and phase-locked oscillations in the growth of a single-species population over a patchy environment. Open Syst. Inf. Dyn. **1**, 127–147 (1992)
15. Yuan, Y., Campbell, S.A.: Stability and synchronization of a ring of identical cells with delayed coupling. J. Dyn. Differ. Equ. **16**, 709–744 (2004)